DOI: 10.21062/mft.2024.046 http://www.journalmt.com

Static and Modal Analysis of the Wheel-side Reducer Cover Plate Based on ANSYS

Zhang Yan (0009-0005-4156-1896)
Major in vehicle engineering, Associate Professor at Anhui Vocational College of Defense Technology, Research direction: Automotive Technology, Lu'an, Anhui Province, China, 237011, E-mail: 285944530@qq.com.

The three-point front-mounted electric forklift is an important logistics tool nowadays. The wheel-side reducer is a vital power unit of the electric forklift. The cover plate of the reducer casing, as a key component, bears significant external loads. The cover plate of the casing is prone to deformation under the action of loads, leading to part scrapping and reducing the service life of the entire machine. Additionally, as the cover plate directly connects with the vehicle body, vibrations produced by the electric forklift during operation can affect the working stability of the reducer through the cover plate, reducing its lifespan. When designers design the wheel-side reducer cover plate, they first establish a 3D model of the cover plate using Pro/E. Then, the 3D model is imported into the finite element analysis software ANSYS. By integrating the Newton-Raphson iterative method, the cover plate undergoes static analysis, predicting potential design flaws and proposing corresponding optimization strategies. After several rounds of simulation and optimization, the cover plate meets the usage requirements. Through modal analysis, the inherent frequency of the cover plate is determined. This allows for the assessment of the relationship between the working frequency and inherent frequency, thus facilitating the improvement of the cover plate's design parameters to reduce resonance and noise. Through static and modal analysis, not only is the design cycle of the reducer cover plate shortened and production costs lowered, but resonance is also minimized, enhancing the working stability of the reducer.

Keywords: ANSYS, Wheel-side Reducer, Cover Plate, Static Analysis, Modal Analysis, Optimization

1 Introduction

Due to the rapid growth of the industrial economy, freight transport and warehousing play an increasingly critical role in the economic growth process. The pacing of technologies like freight and warehousing in various operational stages will significantly impact product logistics costs. If the pace is too slow, it's not conducive to cost savings, the circulation speed of goods and funds, or the improvement of economic benefits. In the logistics process, the use of electric forklifts has played a significant role [1]. The three-point front-driven electric forklift has a small turning radius, a relatively large transmission ratio, and a higher ground clearance. The adoption of the wheel-side reducer not only simplifies the structure of the entire electric forklift, reducing its size but also optimizes the power transmission path, enhances the power transmission efficiency, achieving energy-saving and emission reduction effects. The cover plate, a key component of the wheel-side reducer, bears a large load during operation and is prone to deformation. At the same time, the cover plate directly connects with the electric forklift frame, and the vibrations from the forklift during operation can affect the working stability of the reducer through the cover plate [2].

In recent years, scholars at home and abroad have studied the gear mechanism, casing, and cover plate of the electric forklift's wheel-side reducer. Wan Yuanyuan et al. [3] conducted mechanical analysis on the reducer casing and cover plate, completed the analysis through ANSYS, proposed improvement solutions, and solved the sealing problems of the casing and cover plate. Yang Wenwen et al. [4] conducted static analysis on the electric forklift transmission system, modeled and simulated the drive system using AMESIM software, and analyzed the system's various performances. Agrawal et al. [5]. Utilized ANSYS workbench to perform finite element analysis on straight-tooth cylindrical gears, optimizing components that exceeded allowable stress to extend the gear's operational lifespan.

There are many documents researching the gear structure of electric forklift wheel-side reducers, both domestically and internationally. However, in-depth research on the cover plate is lacking. As a covering part of the wheel-side reducer, the cover plate can be easily overlooked by scholars [6]. The cover plate of the wheel-side reducer in this paper is prone to deformation and resonance due to bearing significant external loads and external vibration interference, leading to operational failure. Whether the cover plate can function effectively directly affects the working condition of the wheel-side reducer. Therefore, it's necessary to conduct static and modal analysis on the cover plate to provide a basis for subsequent structural optimization design, enhance the working stability of the wheel-side reducer, and extend its service life [7].

2 Materials and Methods

2.1 Establishment of the three-dimensional model of the reducer cover plate

The reducer is assembled with a planetary gear set inside. One end of the cover plate is connected to the casing with bolts, and the other end is directly connected to the frame on the frame. The power passes through the output shaft through the cover plate. The two-dimensional diagram of the cover plate is shown in Fig. 1. The layout of the cover plate along with its components on the forklift is shown in Fig. 2. The physical object of the cover plate is shown in Fig. 3, and its layout on the forklift is shown in Fig. 4. Reducer cover plate is large in size and consumes more materials. Given economic and lightweight considerations, it is not suitable to adopt high-price, high-density and high-grade steel, such as 45 steel and 60 steel. However, as the cover plate has certain requirement for mechanical property in the working process of reducer, materials with too low mechanical property cannot be used. Thus, HT200 with advantages in price, density, and mechanical property can be selected for the cover plate. The size of cover plate is presented in Table 1.Generally in the form of castings. The reducer cover plate is lightweight, has a simple process, and is widely used.

Tab. 1 *The size of cover plate*

Material	HT200
Hardness	HB170-230
Length	191.3 mm
Thickness	44.7 mm
Width	187.5 mm
Inner radius	30.8 mm
Outer radius	32 mm
Screw hole radius	10 mm

The structure and usage requirements of the three-point electric forklift determine the characteristics of the reducer cover plate. As the storage spaces such as workshops and warehouses are getting smaller, it is desirable that the size of the forklift is as small as possible. Given this situation, as an important component of the forklift, the size of the wheel-side reducer's cover plate is also required to be as small as possible. Moreover, it is required that the body's own weight cannot be too heavy. The weight of the cover plate accounts for a large proportion of the entire reducer's weight. Therefore, to achieve lightweighting, the weight of the cover plate is an important issue to focus on. In summary, the objectives that the cover plate aims to achieve are lightweight, high strength, small size, and compact structure [8].

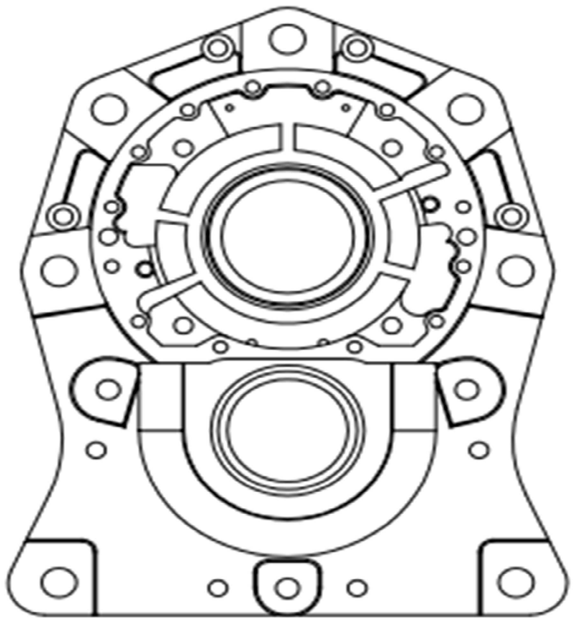

Fig. 1 *Two-dimensional Diagram of the Cover Plate*

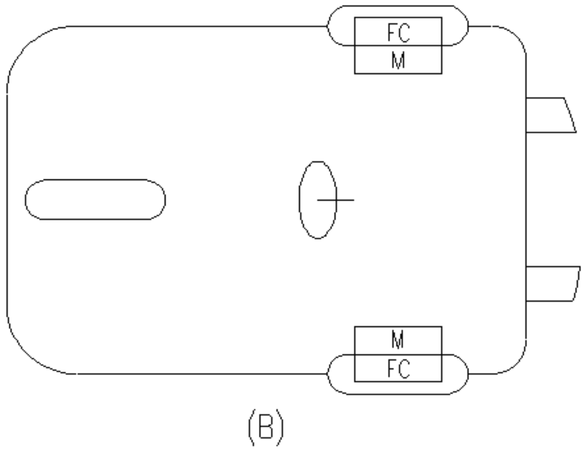

Fig. 2 *Electric Forklift Structure Diagram (M: Motor, FC: Reducer)*

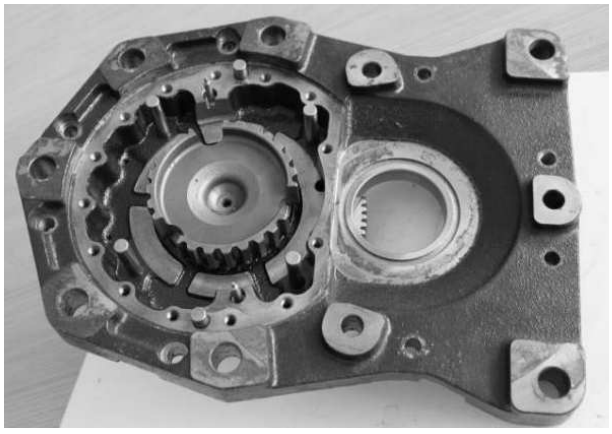

Fig. 3 *Physical Object of the Cover Plate*

Fig. 4 *The Cover and Component Layout Physical Diagram*

A two-dimensional schematic can only provide reference drawings for the production process department when formulating the process flow, but for finite element analysis, the two-dimensional schematic does not meet the needs. Therefore, to complete the finite element analysis, it is necessary to establish a three-dimensional model of the reducer cover plate on the premise of making a two-dimensional schematic [9].

The reducer cover plate and several components connected to the cover plate adopt the method of parametric modeling, using the three-dimensional modeling software Pro/E to establish the three-dimensional model. The modeling steps are shown in Fig. 5:

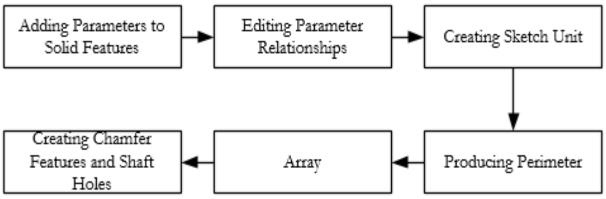

Fig. 5 *Steps for Three-dimensional Modeling*

Through the above steps, the following three-dimensional models were created, as shown in Figs. 6 and 7:

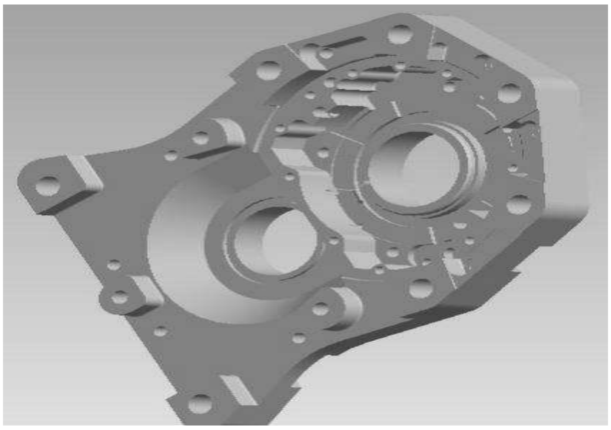

Fig. 6 *Three-dimensional Diagram of the Cover Plate*

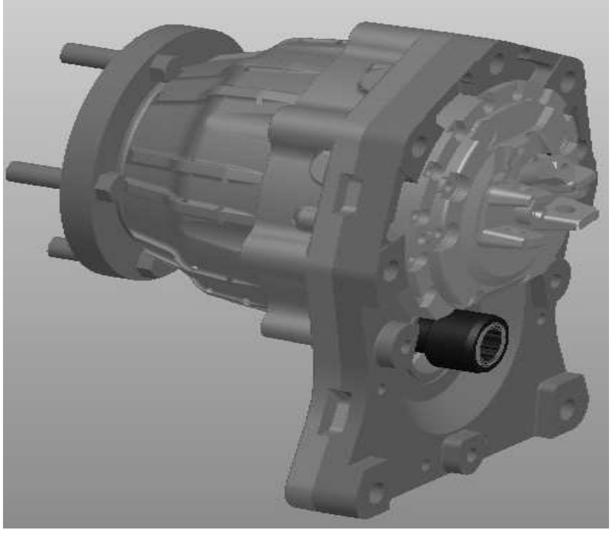

Fig. 7 *The Cover Three-dimensional Diagram*

Considering the structural features of the cover plate, based on the two-dimensional CAD model, a three-dimensional solid model of the cover plate is constructed using large-scale three-dimensional modeling software, which provides a geometric model for the finite element analysis of the cover plate [10].

2.2 Finite element model establishment

First, the model is imported into the finite element environment. It's important to note that during the solid model construction process, the subsequent requirements of finite element analysis software were taken as a basis for modeling. The model is constructed as shown in Fig. 8. With the assistance of data transfer between Pro/E and the general finite element analysis software Ansys, the Cover 3D model is imported.

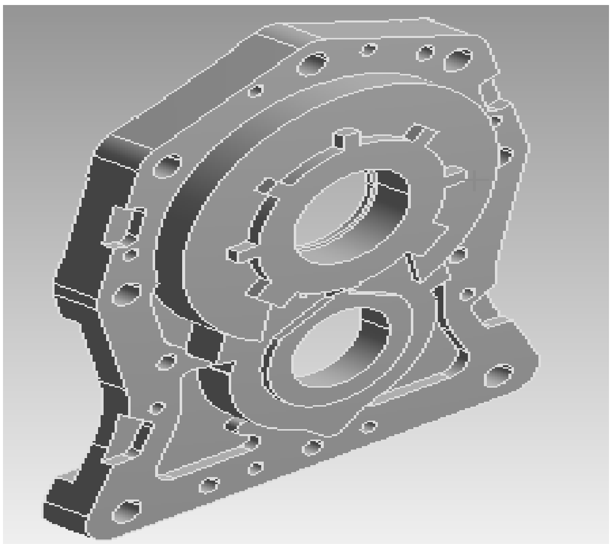

Fig. 8 *3D Solid Model of the Gearbox Cover*

Under the ANSYS environment, first determine the element type to be a 20-node higher-order solid element SOLID95, then define the material properties. Table 2 shows the related properties of the cover material. Based on the above foundation, complete the finite element mesh division of the cover model, creating the gearbox cover finite element model. [11]

Tab. 2 *Parameters Related to the Gearbox Cover*

Material	HT200	**Stress Limit**	182.3 MPa
Max Strain	1.5e-3 mm	**Poisson's Ratio**	0.25
Density	7.8 g/cm³	**Young's Modulus**	150 GPa
Gravitational Acceleration	9.8 m/s²		

ANSYS provides three mesh division methods: free division, mapped division, and sweeping division [12]. The coarseness and method of meshing will greatly influence the accuracy of the results. It's challenging to balance precision and efficiency during finite element simulation of the cover. To enhance precision, increasing mesh quantity adds to the calculation, causing computer crashes. Therefore, while ensuring computational space, optimize meshing to maximize calculation accuracy. In this analysis, sweeping mode is used for the cover meshing. After mesh division, the cover model is shown in Fig. 9 with 25,555 nodes and 14,229 elements.

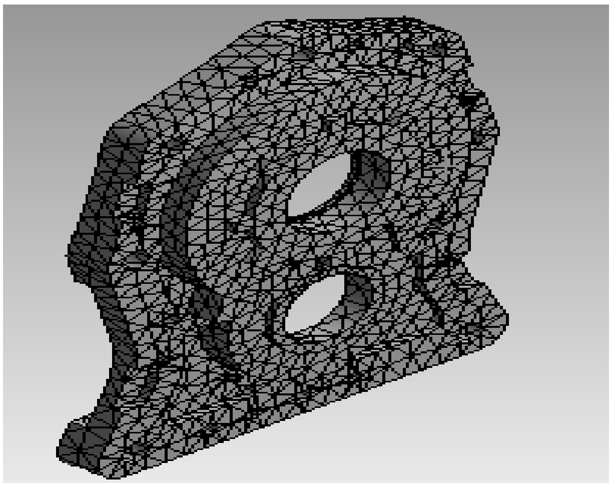

Fig. 9 *Finite Element Model of the Gearbox Cover*

3 Discussion of results

3.1 Static analysis of the cover

3.1.1 Definition of boundary and Loading

After establishing the finite element model, based on the actual placement of the cover on the forklift, six degrees of freedom were constrained on the large end face consolidated with the frame, and all six degrees of freedom were also constrained on the bearing hole mated with the output shaft, ensuring no motion of the cover during loading [13].

The gearbox cover is connected to the frame with 8 large bolts. The load on the cover mainly consists of the vertical load from the forklift's own weight and load, and the radial load from the internal helical gear of the housing. Considering the actual operation conditions of the three-point electric forklift, the primary focus is on the vertical load acting on the cover. The rated load of the forklift is 2 tons, and its own weight is 3 tons. In real-world applications, the forklift may be overloaded. Therefore, when applying the load, it's crucial to add weight exceeding the rated load. The forklift's own weight and load are evenly distributed on the four wheels, so the load on the cover is 1/4 of the total load. Specific loading settings are shown in Table. 3 and the loading is illustrated in Fig. 10.

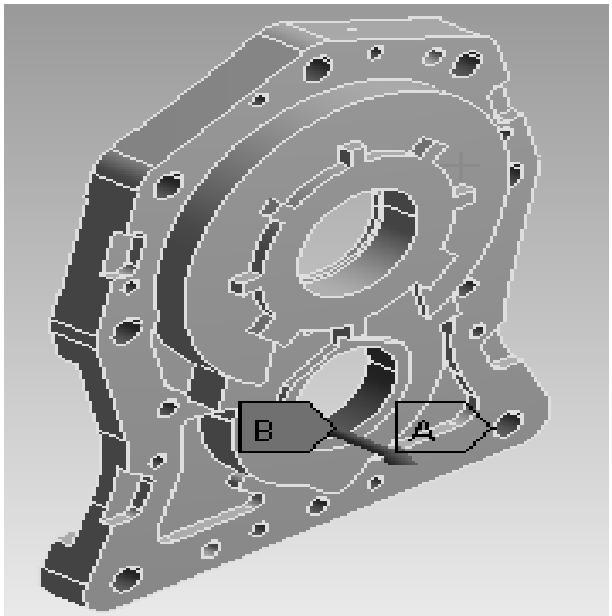

Fig. 10 *Loading Diagram*

Tab. 3 *Cover plate loading*

Type	Details
Load Application Location	Applied on the inner ring of the bearing in contact with the output shaft
Load Application Method	Applied concentrated force
Load Magnitude	No-load: 18620 N, Full-load: 28420 N.

3.1.2 Solution Results

Before solving, set parameters as shown in Table 4:

***Tab. 4** Parameter Settings*

Deformation Mode	Large Displacement Static
Solution Time	1
Number of Substeps	20
Maximum Substeps	50
Line Search	On
DOF solution predictor	On for all substep

***Fig. 11** Full-load Stress Distribution of the Cover*

***Fig. 12** Full-load Strain on the Cover*

After solving, the following results were obtained: For the full-load condition, the stress distribution of the cover is shown in Fig. 11, with the maximum equivalent stress of 204.18MPa occurring on the upper part of the bearing inner ring in contact with the output shaft. The strain on the cover is shown in Fig.12, with the maximum strain of 1.7e-3mm, and the maximum deformation occurring on the upper part of the bearing inner ring. Under no-load conditions, the stress distribution of the cover is shown in Fig. 13, with the maximum equivalent stress of 133.77MPa occurring on the upper part of the bearing inner ring in contact with the output shaft. The strain on the cover is shown in Fig. 14, with the maximum strain of 1.1e-3mm, and the maximum deformation occurring on the upper part of the bearing inner ring.

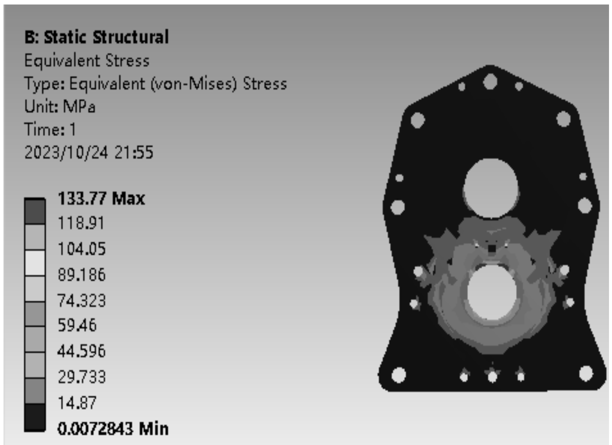

***Fig. 13** No-load Stress Distribution of the Cover*

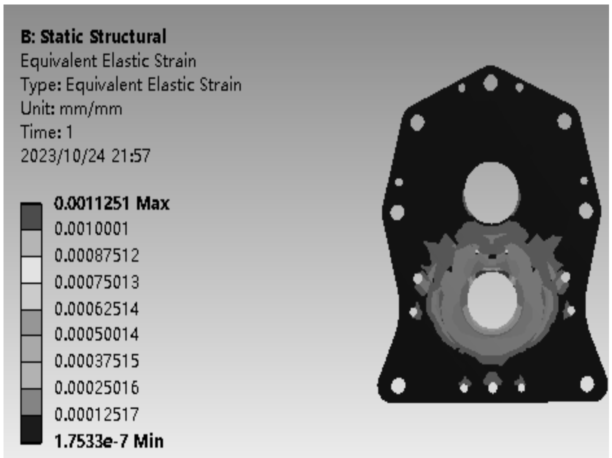

***Fig. 14** No-load Strain on the Cover*

3.1.3 Analysis of computational results

Based on the computational results, it is evident that after applying the respective constraints and loads, the maximum equivalent stress and strain both appear under full-load conditions, with a stress value of 204.18MPa and a strain of 1.7e-3mm. The maximum stress and maximum deformation both occur at the upper part of the inner ring of the bearing. For the no-load condition, the maximum stress is 133.77MPa and the strain is 1.1e-3mm. According to the material data requirements in Table 1, under no-load conditions, both the stress and strain are within the allowable range for the material. However, under full-load conditions, both the stress and deformation exceed the permissible range. If the forklift operates for prolonged periods, it does not meet the material requirements. As a result, the cover plate is prone to deformation and damage from the applied forces, leading to complete machine failure.

3.2 Cover plate optimization and improvement

Analysis under full-load conditions revealed that the maximum values for stress and strain are concentrated at the upper part of the inner ring of the bearing where the cover plate interacts with the output shaft. Thus, by optimizing the dimensions and structure of the cover plate, and then conducting another finite element analysis using ANSYS on these improvements, better results can be achieved. Literature suggests two general approaches for optimization: changing the size of the bearing's inner ring or increasing its thickness. Analysis indicates that the first method is not very feasible because changing the inner ring size would also require changing the size of the mating output shaft. Since this entails broad size modifications, the second method of increasing the thickness is a better choice [14]. The original thickness of the bearing inner ring is 10mm; it can be increased by 2-3mm. However, it is not advisable to increase it too much, as it would add to the weight of the cover plate, which is counterproductive for the lightweighting of the forklift's reducer. After these optimizations, the improved model was recalculated under full-load conditions, yielding the following results:

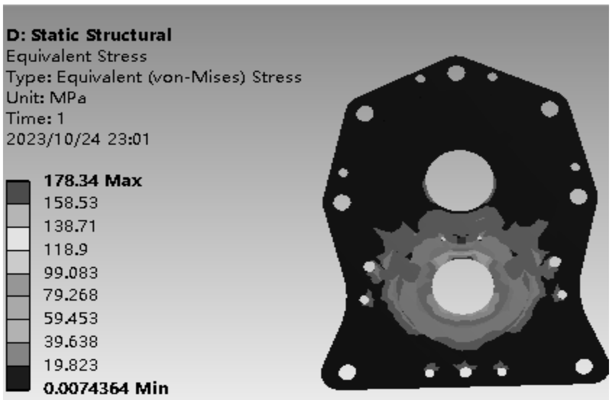

Fig. 15 *Full-load Cover Stress Contour*

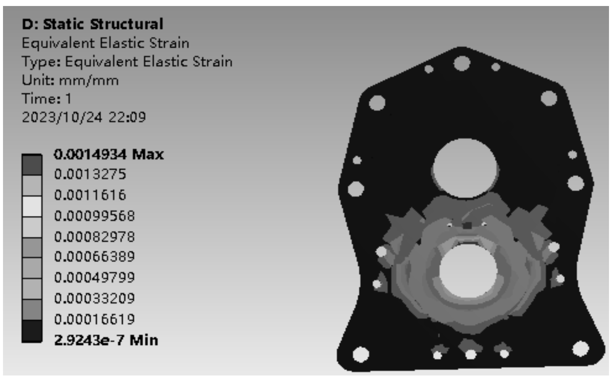

Fig. 16 *Full-load Cover Strain Map*

As shown in Fig. 15 and 16, after dimensional optimization, the maximum stress under full-load conditions is reduced to 178.34 MPa, and the maximum deformation is 1.4e-3mm, meeting operational requirements. Although optimization has reduced the strain, its value is still close to the maximum allowable strain, suggesting that the rigidity of the cover plate should still be enhanced [15].

3.3 Modal analysis of the cover plate

Inherent frequency, also called natural frequency, refers to the specific frequency determined only by the nature of the system when the structural system produces movement under the excitation of the outside world. When the inherent frequency of the wheel reducer cover plate aligns with the working frequency or external excitation frequency, the resonance will bring intense vibration and noise to the reducer, thereby influencing the operation stability of the electric forklift. By analyzing the features of inherent frequency of the cover plate, it is possible to improve the structure at the early stage of product design and avoid occurrence of resonance.

Modal analysis is used to determine the natural frequencies of components so that during design, these frequencies can be avoided or minimized, thereby eliminating excessive vibrations and noise [16]. Through a series of operations, including importing the 3D model diagram from Pro/E, defining material parameters, and setting boundary conditions, the parameters for the cover plate's finite element structural model were established [17]. Using the modal analysis module in the ANSYS software, the cover plate was analyzed. The first 18 constrained modes of the cover plate were calculated, resulting in the natural frequency chart (Fig. 17) for each of these modes. The chart reveals that the natural frequency of the cover plate is relatively high, with the lowest frequency being 4179 Hz. From the 1st to the 18th mode, there's an upward trend in the natural frequencies [18-21].

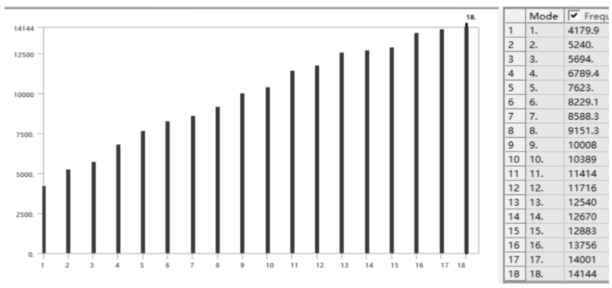

Fig. 17 *Cover Plate Natural Frequencies*

Using the ANSYS modal analysis module, the cover plate was analyzed under actual working conditions. A particular focus was on the displacement of the 10th node, which exhibits the most significant displacement on the cover plate, under the influence of the 1st to 18th mode. Fig. 18-20 show the amplitude and frequency of this node in the X, Y, and Z directions [22].

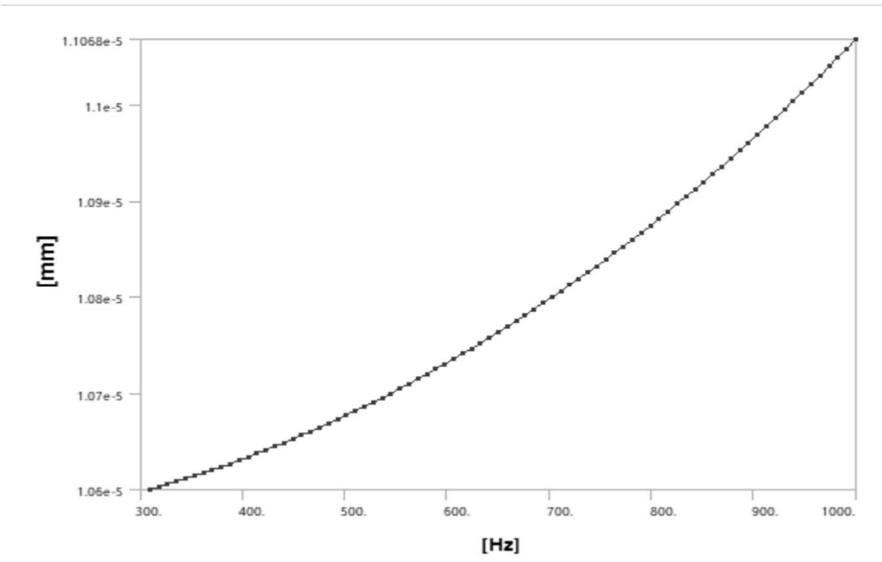

	Frequency [Hz]	Amplitude [mm]
1	308.75	1.06e-005
2	317.5	1.0603e-005
3	326.25	1.0606e-005
4	335.	1.0609e-005
5	343.75	1.0612e-005
6	352.5	1.0615e-005
7	361.25	1.0618e-005
8	370.	1.0621e-005
9	378.75	1.0624e-005
10	387.5	1.0627e-005
11	396.25	1.0631e-005
12	405.	1.0634e-005
13	413.75	1.0638e-005
14	422.5	1.0641e-005
15	431.25	1.0645e-005
16	440.	1.0649e-005
17	448.75	1.0653e-005
18	457.5	1.0656e-005
19	466.25	1.066e-005
20	475.	1.0665e-005

Fig. 18 *X-direction Displacement Chart*

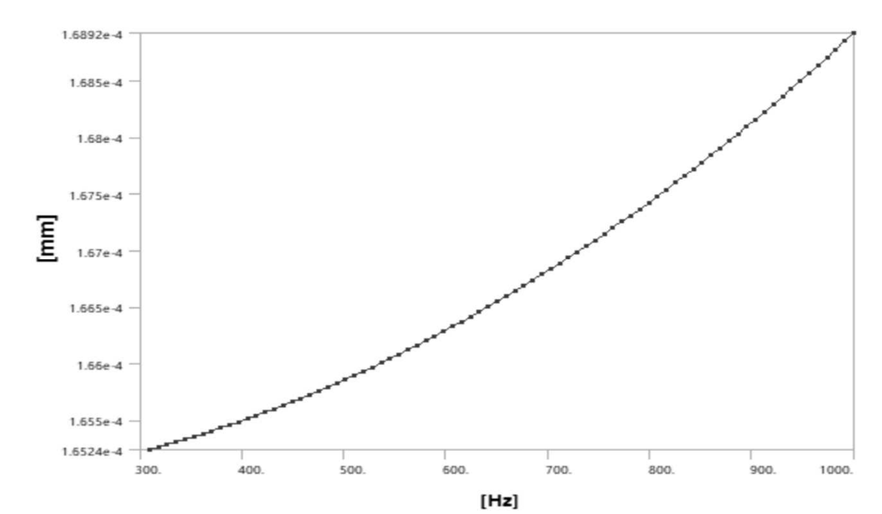

	Frequency [Hz]	Amplitude [mm]
1	308.75	1.6524e-004
2	317.5	1.6526e-004
3	326.25	1.6528e-004
4	335.	1.6531e-004
5	343.75	1.6533e-004
6	352.5	1.6535e-004
7	361.25	1.6538e-004
8	370.	1.654e-004
9	378.75	1.6543e-004
10	387.5	1.6546e-004
11	396.25	1.6548e-004
12	405.	1.6551e-004
13	413.75	1.6554e-004
14	422.5	1.6557e-004
15	431.25	1.656e-004
16	440.	1.6563e-004
17	448.75	1.6566e-004
18	457.5	1.6569e-004
19	466.25	1.6572e-004
20	475.	1.6576e-004

Fig. 19 *Y-direction Displacement Chart*

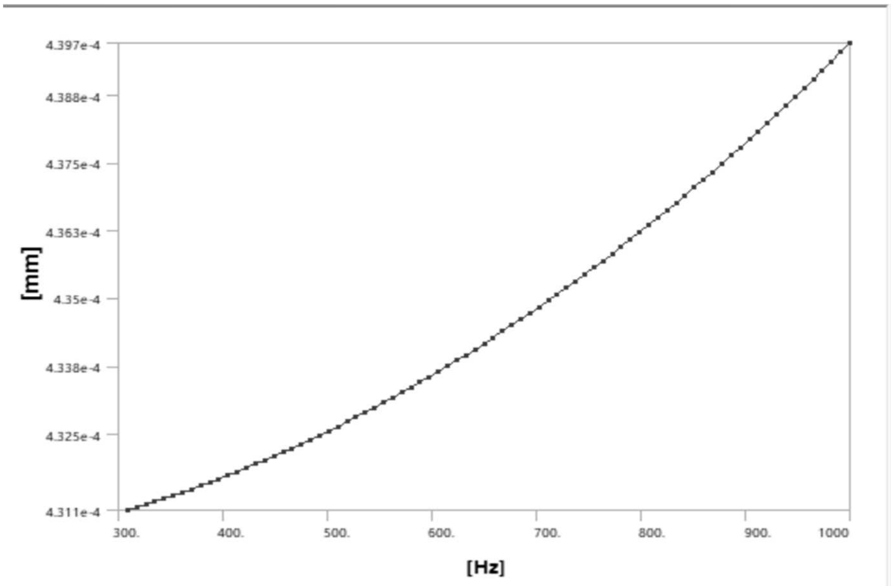

	Frequency [Hz]	Amplitude [mm]
1	308.75	4.311e-004
2	317.5	4.3115e-004
3	326.25	4.312e-004
4	335.	4.3126e-004
5	343.75	4.3131e-004
6	352.5	4.3137e-004
7	361.25	4.3143e-004
8	370.	4.3149e-004
9	378.75	4.3155e-004
10	387.5	4.3161e-004
11	396.25	4.3167e-004
12	405.	4.3174e-004
13	413.75	4.3181e-004
14	422.5	4.3188e-004
15	431.25	4.3195e-004
16	440.	4.3202e-004
17	448.75	4.3209e-004
18	457.5	4.3216e-004
19	466.25	4.3224e-004
20	475.	4.3232e-004

Fig. 20 *Z-direction Displacement Chart*

For the cover plate, when its vibration frequency matches its natural frequency, the amplitude of the vibration greatly exceeds its allowable displacement, leading to structural damage and directly affecting the normal operation of the wheel-side reducer. Analysis of the cover plate's natural frequency and the displacement curves of the 10th node with mode changes reveal that, as the node with the most considerable displacement on the cover plate, its vibration frequency gradually increases from the 1st to the 18th mode. The highest frequency is 475Hz, significantly lower than the cover plate's lowest natural frequency of 4179Hz. In every mode, the vibration frequency is much lower than the cover plate's natural frequency, so the likelihood of resonance occurring during actual operation is very low [23]. If resonance does occur in the cover plate, analyzing the frequencies and modes can help avoid the cover plate operating at the resonance frequency over the long term by changing the material rigidity and structural form, which can enhance the lifespan of the wheel-side reducer.

4 Conclusions

With the rapid advancement and widespread use of mathematical theories and computer technology, finite element analysis has also seen swift progress. ANSYS software integrates analysis of structures, fluids, electric fields, magnetic fields, and acoustic fields, making it a comprehensive general-purpose finite element analysis tool. ANSYS is now widely used in modern engineering analysis. Currently, the finite element method has become an indispensable technology and analysis tool in both engineering design and research domains, addressing numerous practical issues and contributing significantly to the national economy. This paper has utilized ANSYS to analyze and research the key component of the wheel-side reducer, the cover plate, providing vital data support for the design, optimization, and manufacturing of electric forklift braking systems.

Using material performance requirements as a basis, finite element analysis revealed that the stresses and strains on the cover plate under full-load conditions do not meet material requirements. Drawing upon scholarly expertise, the dimensions of the cover plate were optimized. The optimized cover plate's stresses and deformations were all within the specified range, thus completing the static analysis of the reducer's cover plate. Moreover, to prevent the adverse effects of vibration on the wheel-side reducer during the operation of electric forklifts, a modal analysis was conducted on the cover plate, which is the component most closely connected to the electric forklift. The analysis concluded that the working frequency is much lower than the cover plate's natural frequency, making the likelihood of resonance extremely low. As an essential part of the wheel-side reducer, the cover plate's static and modal analysis results have been used to make further improvements and optimizations, greatly enhancing the reliability of the wheel-side reducer and extending the lifespan of electric forklifts. This paper only presents static and modal analyses of the cover plate under standard operating conditions. Besides standard operations, real-world forklift operations include braking and turning conditions. Analyses of these two conditions will be the focus of future work. Subsequent analyses aim to provide a more comprehensive data set, offering greater guidance for the design and manufacturing of the wheel-side reducer.

Acknowledgement

This work was supported by the 2023 Key Research Projects of the College (gf2023jxyjz02) and the 2023 Anhui Province Vocational Education Project (AZCJ2023024).

References

[1] WAN, Y., (2016). Dynamic Contact Simulation Study of Wheel-side Reducer Gear. In: *Computer Simulation,* Vol. 4, pp. 260-264.

[2] WU, X., (2013). Design and Analysis of a Wheel-side Reducer with Wet Braking Function. In: *Mechanical Engineering & Automation,* Vol. 4, pp. 33-35.

[3] WAN, Y., PENG, Q., YU, F., (2023). Optimization and Verification of Sealing Design for Electric Forklift Reducer Casing. In: *Construction Machinery,* Vol. 54, No. 6, pp. 177-181.

[4] YANG, W., KE, J., YANG, Z., et al. (2020). Design and Simulation Study of Electric Forklift Hydrostatic Drive System. In: *Machine Tool & Hydraulics,* Vol. 48, No. 2, pp. 71-75.

[5] AGRAWAL, A.P., ALI, S., RATHORE, S., (2022). Finite element stress analysis for shape optimization of spur gear using ANSYS. In: *Materials Today: Proceedings,* Vol. 64, No. 3, pp. 1147-1152.

[6] KATRIN, B., HERMANN, F., (2023). Modelling and Simulation of Aerodynamic Cylindrical Bearings Using ANSYS Hydrodynamic Bearing Element Types. In: *Vehicles,* Vol. 5, No. 3, pp. 1118-1132.

[7] CAI, X., (2016). Failure Analysis of Frame Fracture of Mine Dump Truck Wheel-side Reducer. Coal. In: *Mine Machinery,* Vol. 3, pp. 70-72.

[8] SHI, F., (2018). Vibration Control of Reciprocating Compressor and Application of Airflow Pulsation Method. In: *Engineering Construction and Design,* Vol. 15, pp. 83-85.

[9] ZHANG, Z., FENG, G., SUN, H., et al. (2020). Rigid-Flexible Coupling Modeling and Load Characteristics Study of Gear Transmission System. In: *Mechanical Strength,* Vol. 42, No. 1, pp. 239-245.

[10] YANG, S., LIU, X., ZHANG, L. et al. (2023). Analysis of Wheel-side Reducer Gear Temperature Field and Contact Fatigue Life for Loaders. In: *Mechanical Design & Research,* Vol. 39, No. 1, pp. 82-86.

[11] FERNANDES, C.M., DIOGO, R., MARTINSR, C., et al. (2018). Finite element method model to predict bulk and flash temperatures on polymer gears. In: *Tribology International,* Vol. 120, No. 12, pp. 255-268.

[12] GUILLERMO, E., MORALES, E., ANTONIO, G., (2018). A model for gear life with surface and subsurface survival: Tribological effects. In: *Wear,* Vol. 404-405, pp. 133-142.

[13] QU, W., FAN, Z., CHEN, L., et al. (2022). Dynamic Contact Characteristics Study of Planetary Wheel-side Reducer. In: *Mechanical and Electrical Engineering,* Vol. 39, No. 2, pp. 224-230.

[14] NABAWY, A.E., ABDELRAHMAN, A.A., ABDALLA, W.S., et al. (2019). Analysis of the dynamic behavior of the double wishbone suspension system. In: *International Journal of Applied Mechanics,* Vol. 11, No. 34, pp. 1 - 19.

[15] EBRAHIMI, M., BUTSCHER, A., CHEONG, H., et al. (2019). Design optimization of dynamic flexible multibody systems using the discrete adjoint variable method. In: *Computers & Structures,* Vol. 213, No. 3, pp. 82-99.

[16] P. WEIS, Ľ. KUČERA, P. PECHÁČ, M. MOČILAN, (2017). Modal Analysis of Gearbox Housing with Applied Load. In: *Procedia Engineering,* Vol. 192, pp. 953– 958.

[17] LYASHENKO, M.V., CHEBANENKO, A.P., POTAPOV, P.V., (2017). Analysis of Stresses in Elements of Hub Reduction Gear of TREKOL-39041Off-road Vehicle. In: *Procedia Engineering,* Vol. 206, pp. 1564-1569.

[18] AHIWALE, D., MADAKE, H., et al. (2022). Modal analysis of cracked cantilever beam using ANSYS software. In: *Materials Today: Proceedings,* Vol. 56, No. 1, pp. 165-170.

[19] KRMELA, J., BERLADIR, K., POZOVNYI, O., ARTYUKHOVA, N. (2022). Erosion Modelling of Structural Materials in the Working Space of Multistage Convective Dryers. *Manufacturing Technology*, 22, 307-318.

[20] CEDZO, M., JOCH, R., TIMKO, P., HOLUBJÁK, J., CZÁNOVÁ, T., ŠAJGALÍK, M. (2023). Topology Optimization of Gripping Jaws of Industrial Robot. *Manufacturing Technology*, 23, 25-31.

[21] JIN, X., ZHANG, X., CHENG, Z., LI, Y., FAN, B., CHEN, X., WANG, X., WANG, M. (2023). Exploration of Key Technologies of Intelligent Inspection Robots in the Application of Automatic Energy Meter Verification Line. *Manufacturing Technology*, 23, 426-435.

[22] SHASHI, K.G., KRISHNAPPA, G.B., (2022). Design and finite element analysis of AISI 4340 alloy steel helical gear. In: *Materials Today: Proceedings*, Vol. 65, No. 8, pp.3671-3674.

[23] PAVAN KISHORE, M.L., SREENIVASULU, B., RAGHU KUMAR REDDY, B.C., (2017). Modal Analysis of Rectangular Plate with Central Hole Subjected to Various End Conditions. In: *Materials Today: Proceedings,* Vol. 4, No. 2, pp.1653-1663.